Hindawi
Advances in Civil Engineering
Volume 2018, Article ID 6275941, 18 pages
https://doi.org/10.1155/2018/6275941

Research Article

Stability of Close Chambers Surrounding Rock in Deep and Comprehensive Control Technology

Weijian Yu[1,2] **and Fangfang Liu**[1]

[1]*School of Resource and Environment and Safety Engineering, Hunan University of Science and Technology, Xiangtan, Hunan 411201, China*
[2]*Hunan Key Laboratory of Safe Mining Techniques of Coal Mines, Hunan University of Science and Technology, Xiangtan, Hunan 411201, China*

Correspondence should be addressed to Weijian Yu; ywjlah@163.com

Received 25 April 2018; Accepted 4 July 2018; Published 28 August 2018

Academic Editor: Fengqiang Gong

The purpose of this paper is to solve the problem that deep and close-distance cavern and roadway group were easily affected by the adjacent chamber or roadway excavation disturbance and low stability and significant deformation of surrounding rock occurred. The stability and control technology of surrounding rock in the main shaft and auxiliary shaft system has been analyzed by the adjacent chamber and roadway group of −850 m level in Qujiang Mine, China, as an engineering background. Firstly, the numerical calculation of the excavation chamber was, respectively, carried out in different ways with the propagation theory of the excavation disturbance wave. The results show that the interaction of adjacent chamber excavation was more intense. When excavated at the same time, there is a large increase in the movement of the sides and the roof-floor of the chamber and roadway. Then, the mechanism of interaction between low-high stress and excavation disturbance was considered, the corresponding control principles were provided, and a set of critical technologies and equipment were designed according to the deformation characteristics of the large deformation soft surrounding rock. Finally, the comprehensive control method was put forward with the water pump house as an example, that is, anchor, metal net, grouting, combined anchor cable and large-diameter anchor cable. And the related support parameters were determined by the internal damage of the surrounding rock chamber. The numerical simulation results show that the surrounding rock deformation of the chamber and roadway reduced with the revised support program, which the expansion of the rock mass loose circle prevented effectively. The site test shows that the convergence rate of surrounding rock with the improved support was less than 0.2 mm/d, and the rock deformation of chamber and roadway suppressed significantly.

1. Introduction

Many chambers and roadways are arranged tightly in the mine construction and form a denser chamber group. The influence between the dense chambers is intense, and the stability of a chamber or roadway is mainly affected by the excavation disturbance and the superposition of stress, during an excavation of the chamber or roadway [1–3]. Especially for a production mine, the main and auxiliary shaft system and chambers are the central passageways of mine production and the critical engineering of safe and efficient mining. Therefore, the stability of surrounding rock is worth studying in a short-distance chamber or roadway under the action of low-high stress. At present, scholars at home and abroad have carried out a series of studies and obtained more achievements on the stability and control of surrounding rock in deep and close-distance chambers [4–6]. Among them, block theory, ant colony algorithm, numerical calculation, and other methods have been applied in the stability analysis and construction optimization of surrounding rock of the chamber group [7–9]. Yang et al. analyzed the influence of chamber group excavation on the distribution range of surrounding rock stress and plastic zone of the chamber group and surrounding roadway [10].

Lin and Shi analyzed the deformation and failure of the large-section chamber surrounding rock in a deep and complex structure area and put forward the stability control strategy of the bolt-mesh-cable-coupled coupling support [11]. Yang et al. analyzed the stability of the underground chamber surrounding rock of the desolate hydropower station by using the block theory that is suitable for the stability analysis of the fractured rock mass [12]. Zhao et al. performed rock creep tests under multilevel load and revealed the nonlinear relationships between the instantaneous strain, viscoelastic strain, viscoplastic strain, and high deviatoric stress [13]. Sun et al. analyzed the instability process under the influence of mining movement, aiming at the instability and destruction of −670 m pump chamber group in the initial secondary recovery of Nantun Coal Mine, China [14]. Wang et al. adopted the pump chamber group of no. 42 mining area in Peigou Coal Mine, China, as the research object. The development of the surrounding rock loose circle for the chamber group is detected by using the geological radar and drilling peers. The technology of cooperating support and anchor net cable control was put forward [15]. He et al. used FLAC^{3D} to study the mechanical response and deformation characteristics of different displacement deformation and stress states, which are caused by different excavation sequences of grade separation chamber rock in the deep soft rock roadway [16]. Kang et al. researched the stress distribution and comprehensive reinforcement technology of the loose and fractured chamber group surrounding rock in the shaft station of Lu'an Tunliu Mine, Shanxi, China. A comprehensive reinforcement method for loosely broken rock, that is, high prestressing, strong bolt, and anchor support after high-pressure grouting, was proposed [17]. Wang et al. analyzed the main reasons and control factors for the critical parts destruction of the pump room and chamber group with the traditional arrangement form. The coupling support technology, that is, anchor net cable + truss + bottom angle grouting anchor pipe, was proposed [18].

Above research results provide an essential reference for the study of the stability and control of surrounding rock in the deep chamber group and play a signification guiding role in the safe and efficient mining. However, the excavation of adjacent chambers or roadways destroyed original surrounding rock directly and the stability of the surrounding rock of each chamber or roadway significantly, with the effect of stress concentration. The universal phenomenon of roof sinking, bulging, and floor cracking or bulging is bringing great difficulties for the production of Qujiang Coal Mine, Jiangxi, China. Therefore, this paper is aimed at the close-distance cavern and roadway group at −850 m level in Qujiang Coal Mine; the stability analysis of surrounding rock of the main and auxiliary shaft system was carried out, and the corresponding control technology was put forward.

2. Project Overview and the Original Design Support Program

The depth of the −850 m main shaft in Jiangxi Qujiang Coal Mine is 886 m. The main chamber roadway includes the main shaft and auxiliary shaft, central substation, water pump house, waiting room, main haulageway, and passby roadway. The layout and section layout are shown in Figure 1(a). The rock mass of the chamber and roadway is mudstone or silty nearly, grayish black, and thin-to-medium thick layer, sandwiched with thin layers of mudstone and fine sandstone, with little siderite nodules. The stratum contains plant roots fossils, joint development, and calcium mud cementation with medium to low hardness.

The plane of the waiting room, −850 m main haulageway, and water pump house chamber were taken as the research subject (Figure (1b)). The two-excavation and one-spray procedure of the three-eight system was carried out for full-section excavation by the drilling and blasting method in the chamber. The composed control method of the anchor, beam, net, and grouting reinforcement is adopted in the original design of the waiting chamber. The anchor supporting material was the same-strength rebar bolt, with 20 mm diameter × 2000 mm length and 800 mm × 800 mm spacing.

The section of the passby roadway lane, main haulageway, central substation, and main pump are the semicircular arch. The anchor, beam, mesh, anchor cable, and shotcrete support are adopted, and U29 metal support is added in the broken zone. All of them, the anchor supporting material was the same-strength rebar bolt. The bolt specification of the passby roadway lane and main haulageway was 20 mm diameter × 2500 mm length, with the spacing of 800 mm × 800 mm. The bolt of the central substation and the main pump was of 20 mm diameter × 2500 mm length, with the spacing of 800 mm × 800 mm, and the anchor cable was a stranded wire of 15.24 mm diameter × 7000 mm length, with the spacing of 2000 mm × 1600 mm, respectively. The specific section and location of each chamber are shown in Figure 1(b).

3. Numerical Analysis of the Disturbance Effect on Site Construction

3.1. Rock Mechanical Strength Analysis. Six samples of siltstone rock were collected for uniaxial compression tests in the bottom chamber and roadway of the central well at −850 m Quijano Coal Mine [19]. The compressive and elastic deformation stages of rock samples before achieving peak strength were similar, and the yield stages were different. The apparent strain was the softening phenomenon in some rock masses, but most specimens were the brittle failure. The results of the uniaxial compression test are shown in Table 1; the minimum, maximum, and average uniaxial compressive strength of the rock specimen were 23.37 MPa, 67.50 MPa, and 48.74 MPa, respectively. Therefore, the differences in mechanical properties of rocks were noticeable. Uniaxial test failure results of some rock specimens are shown in Figure 2. Extreme development of tectonic fractures was in the area where the sampled rocks are located, and there were significant differences in the dispersion of rock specimens at the same sampling point. The distribution of primary fractures was different (Figure 2(a)); when the rock in the same area was subjected to shear failure, there was no apparent

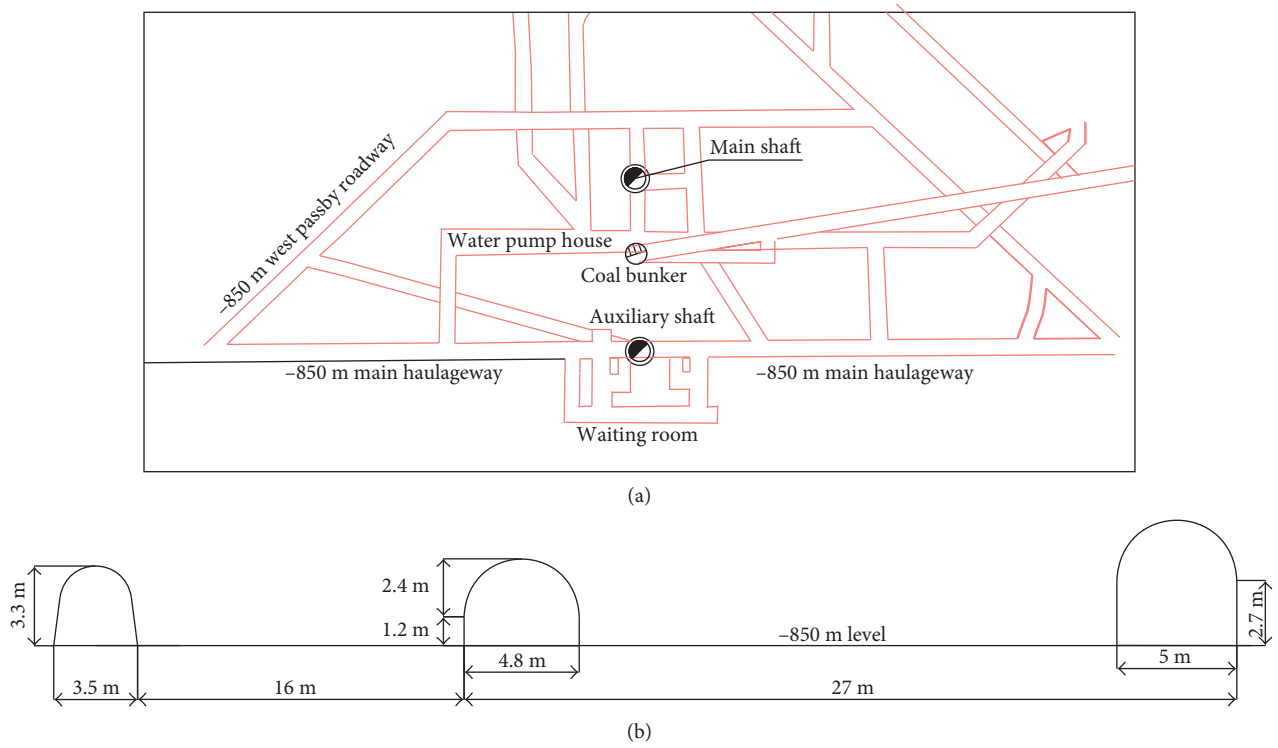

Figure 1: Chamber group layout plan. (a) Shaft station chamber and roadway layout plan. (b) Position relationship of the pump room, transport lane, and waiting room.

Table 1: Test results of uniaxial compressive strength.

Sample category	Number	Compression strength (MPa)	Elastic modulus (GPa)	Poisson's ratio	Average compressive strength (MPa)	Average elastic modulus (GPa)	Average Poisson's ratio
Siltstone	B1-1	42.75	4.62	0.39	48.23	5.88	0.36
	B1-2	53.71	7.14	0.23			
	G1-1	23.37	9.66	0.27	31.62	7.98	0.31
	G1-2	39.88	6.30	0.35			
	J1-1	67.50	1.26	0.47	66.36	2.10	0.45
	J1-2	65.21	2.94	0.43			

difference between the failure law of the secondary fracture and primary fissure because of the similar degree of rock failure (as shown in Figure 2(b)). The test results showed that the mechanical properties of the rock were significantly different. It indicates that the rock mass was greatly affected by the structural plane. That is, the different degrees of crack development result in inconsistent mechanical strength of the rock mass in the same roadway.

3.2. Numerical Simulation Analysis of the Surrounding Rock Stability of the Chamber Group. The field geological data and the mechanical parameters of the roadway surrounding rock were considered, the numerical calculation models were established by FLAC^{2D}, and the model size was 90 m × 50 m. The left, right, and lower boundaries of the model were fixed boundaries with displacement constraints, and the upper boundary was the stress boundary. The uniformly distributed load was applied by the overlying strata thickness. The lower boundary was 920 m above the surface, and the vertical stress of 21.75 MPa was applied on the upper boundary. The Mohr–Coulomb criterion was used in the failure process. The rock formations and the mechanical parameters of the rock strata are shown in Figure 3 and Table 2, respectively.

3.3. Propagation Principle of the Excavation Disturbance Wave. The disturbance stress generated by the explosion can damage and destroy the surrounding rock of the excavation section when the roadway or chamber was blasting excavation. Adverse effects on surrounding rock of the excavation section and nearby cave, the falling or flaking of surrounding rock and even rock burst, were induced [20]. Rocks absorbed disturbed stress waves until they disappear as they propagate in rock media. Therefore, there is a specific attenuation rule for the disturbance wave propagating in the

(a)

(b)

Figure 2: Uniaxial test failure results of some rock specimens: (a) rock samples before destruction; (b) damaged rock sample.

Figure 3: Numerical calculation model of the chamber surrounding rock.

rock when the roadway excavated. In general, the attenuation of the disturbed stress wave in hard rock was less than that in a soft rock during the excavation of the roadway. The attenuation index was related to the strength of rock, and the amplitude attenuation of the disturbance stress wave was usually expressed as follows:

$$s_{r\ \max} = s_{\max}\left[\frac{k}{r_0^n}\right], \tag{1}$$

where $s_{r\ \max}$ is the amplitude of the disturbance wave at the distance r from the blasting heart (MPa); $s_{\max}$ is the amplitude of the disturbed stress wave on the wall of the blast hole (MPa); r_0 is the relative distance, that is, $r_0 = r/R_0$, in which R_0 is the charge radius (m) and r is the distance of the explosive center, that is, the blasting disturbance influence radius (m); and k and n are the coefficients related to the mechanical strength of rock and fitted by static compressive strength values of multiple group rocks, respectively. There is a fitting relationship between k, n, and the static compressive strength s_0 under the rock strength range of 80~100 MPa, as found by the experimental results:

$$k = 631\ \exp\left(\frac{s_0}{6 + 0.26\ s_0}\right),$$
$$n = \frac{31 + 0.79\ s_0}{10 + 0.577\ s_0}. \tag{2}$$

Table 2: Main rock mechanical parameters.

Rock formation name	Volume modulus (GPa)	Shear modulus (GPa)	Density (kg·m^{-3})	Internal friction angle (°)	Bonding force (MPa)	Tensile strength (MPa)
Overburden	9.0	2.4	2500	36.0	2.5	3.7
Sandstone	7.0	2.5	2400	31.5	3.7	3.8
Siltstone	7.0	2.0	2500	31.0	2.5	—
Sandstone	7.0	2.5	2400	31.5	3.7	3.8
Sandy mudstone	6.4	2.4	2300	32.5	1.8	3.5

For the surrounding rock of the mine roadway and chamber under the complex environment, the complex stress distribution and stress concentration of roadways and the surrounding chambers occurred during the short-distance excavation. The dynamic stress generated inside surrounding rock under the action of the excavation disturbance stress wave, and a joint operation of dynamic stress and stress weight was formed, by which the stability of surrounding rock reduced and the possibility of roadway and chamber instability increased.

3.4. Numerical Calculation Results of Deformation Characteristics of the Roadway Surrounding Rock under Excavation Disturbance. In numerical calculation, the deformation of surrounding rock caused by blasting excavation mainly considered the external load and dynamic boundary conditions of the numerical model inputted from the stress disturbance wave. According to the field measurement results, if the interval between two adjacent holes was more significant than 100 ms, the superposition of blasting vibration (i.e., interference of the stress wave) caused by the explosion of inter-row charge holes cannot be considered when multiple-row hole blasting is used. Therefore, only the most extensive section of the discharge hole is taken as the calculated dose in the calculation. In order to eliminate the acceleration discontinuity caused by the numerical integration method, the load waveform was taken as harmonic in the computation at the excavation of blasting vibration and other dynamic disturbances of rock mass. The mathematical expression was usually expressed as follows:

$$P(t) = \begin{cases} P_{\max}\left[\frac{1}{2} - \frac{1}{2}\cos(2\pi\omega t)\right], & (t \le 1/\omega), \\ 0, & (t > 1/\omega), \end{cases} \quad (3)$$

where $P_{\max}$ is the stress peak of excavation disturbance (MPa), ω is the dynamic loading frequency (Hz), and t is the sustained action time of disturbance stress (ms). According to the characteristics of actual excavation, $P_{\max}$ is 20 MPa, ω is 200 Hz, and t is 5 ms. The time-history curve of the stress wave is shown in Figure 4.

FLAC^{3D} can be applied to simulate the response of the material to external or internal dynamic forces by the dynamic loads applied at the boundary or internal node of the model. The dynamic load input included acceleration-time histories, velocity-time histories, stress-time histories, and force-time histories. After excavation of the roadway model,

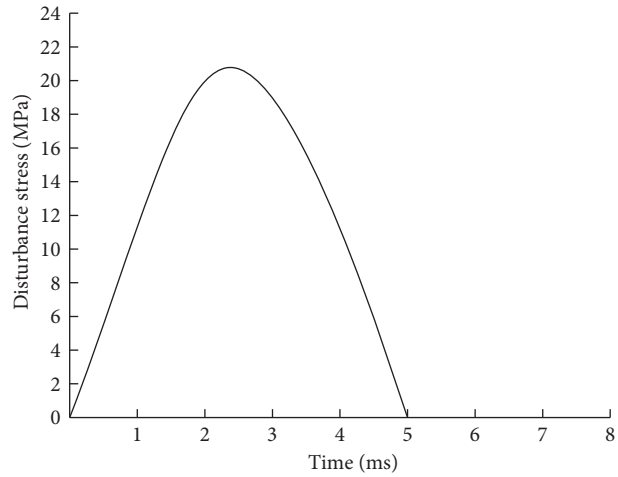

Figure 4: Time-history curve of the blasting disturbance stress wave.

the stress wave was assumed to be perpendicular to the wall of the roadway when the sides, roof, floor, and brace were inputted at the wall of the roadway by stress-time histories.

In addition, the Rayleigh damping was first used in the calculation, with the internal friction of the rock material and the possible sliding of the contact surface considered. Assume that the damping matrix C in the dynamic equation was related to the stiffness matrix K and the mass matrix M:

$$C = \alpha M + \beta K, \quad (4)$$

where α is the damping constant proportional to quality and β is the damping constant proportional to stiffness. In the calculation procedure, the constitutive relation of the critical time step in the dynamic calculation was as follows:

$$\Delta t_{\text{crit}} = \min\left\{\frac{V}{C_p A^f_{\max}}\right\}, \quad (5)$$

where C_p is the longitudinal wave velocity, which is related to the bulk modulus K and the shear modulus G of the material, and can be expressed as $C_p = \sqrt{(K + (4/3)G)/\rho}$ (m/s); V is the volume of the subzone (m^3);$A^f_{\max}$ is the maximum surface area associated with the tetrahedron subzone (m^2); and min{} traverses all elements, including structural elements and contact surface units.

Therefore, according to the theory of excavation disturbance wave propagation, the numerical calculation of the excavating water pump house alone, the excavating water pump house and main haulageway at the same time, and the

Table 3: Deformation of the chamber under different excavation modes (unit: mm).

Excavation mode	Chamber	Floor heave volume	Roof subsidence volume	Left side horizontal displacement	Right side horizontal displacement
Excavation of the water pump house	Water pump house	389	437	549	579
Excavation of the water pump house and transport roadway		524	645	832	719
Excavation of the waiting room, −850 m main haulageway, and water pump house		614	726	959	750
	−850 m main haulageway	662	743	774	789
	Waiting room	509	504	560	662

excavating waiting room, main haulageway, and water pump house at the same time was carried out, respectively, and the results are shown in Table 3. The vertical stress and the plastic zone of surrounding rock during the excavation of the water pump chamber are shown in Figures 5(a) and 5(b), and the vertical stress and the plastic zone of surrounding rock during the excavation of the water pump house and main haulageway are shown in Figures 6(a) and 6(b), respectively.

In contrast, the deformation of the sides and roof-floor was relatively small when the excavation of the water pump house alone is considered. The stress distribution changed while the water pump house and main haulageway are excavated at the same time. Especially, the stress redistribution of surrounding rock was caused by the excavation of the main haulageway, and a higher degree of the stress concentration was reached, by which the convergence of the sides and roof-floor significantly increased and the interaction between excavations of adjacent chambers was relatively intense.

When the waiting room, main haulageway, and water pump house are excavated at the same time, the displacement of the roof-floor or sides was more massive than all in the absence of the bolting and anchoring support. Therefore, the deformation of the water pump house was severe significantly, and the left horizontal displacement of the chamber was substantially higher than the right. The extensive range stress concentration of vertical stress between the water pump house and main haulageway and a sizeable horizontal displacement of surrounding rock near the stress concentration area were formed (Figure 7(a)). The damage range of the surrounding rock chamber and roadway was more extensive, and the loosening circle was larger under the influence of high stress (Figure 7(b)).

4. Comprehensive Control Principle Analysis of High Stress Chamber Rock

4.1. Control Principle. Because of the deformation characteristics of large deformation soft rock, the joint action of deep high stress and excavation disturbance was taken into account; the following control principles were put forward:

(1) The initial support strength of the support system was enhanced, and the integrity of surrounding rock was maintained. The initial support stiffness and strength of the supporting system were significantly improved, and the discontinuous deformation of surrounding rock was controlled effectively. At the same time, the greater continuous deformation of the roadway surrounding rock was supported by the sufficient elongation of the support system that the high stress was released and the influence of excavation disturbance was absorbed. Therefore, compared with the traditional support concept that first soft and rigid afterwards, first yield and resist afterwards, the support sequence of complex roadway in deep was first stiff, then soft and rigid; first resist, then yield and resist. The integrity of surrounding rock was maintained maximally, and the strength of surrounding rock was reduced.

(2) The stress state of surrounding rock was improved, and the self-bearing force of surrounding rock was given a full play. The main function of the prestressed anchor is to control the expansion deformation in the surrounding rock of the anchorage zone, such as dissociation, slip, crack opening, and new crack generation. The surrounding rock was under pressure, and the occurrence of bending deformation, tensile, and shear failure of the surrounding rock was suppressed. The prestressed bearing structure with large stiffness was formed in the anchorage zone, the strata outside the anchorage zone were prevented, and the stress distribution in deep surrounding rock was improved.

(3) The prestress and scope of action of the bolt were effectively improved. The key to the design of the support is to determine the reasonable prestress according to the condition of the roadway and to achieve effective diffusion of the prestress. The range of the single anchor bolt was limited; the prestressed anchor bar must be diffused into the surrounding rock further away from the anchor rod using a supporting plate, steel strip, and metal mesh. Especially for the roadway surface, the deformation and destruction of surrounding rock were inhibited naturally, and the integrity of roof was maintained, even if a small supporting force was applied. Anchor plate, steel band, metal mesh, and other watch components play an extremely important role in the prestressed support system.

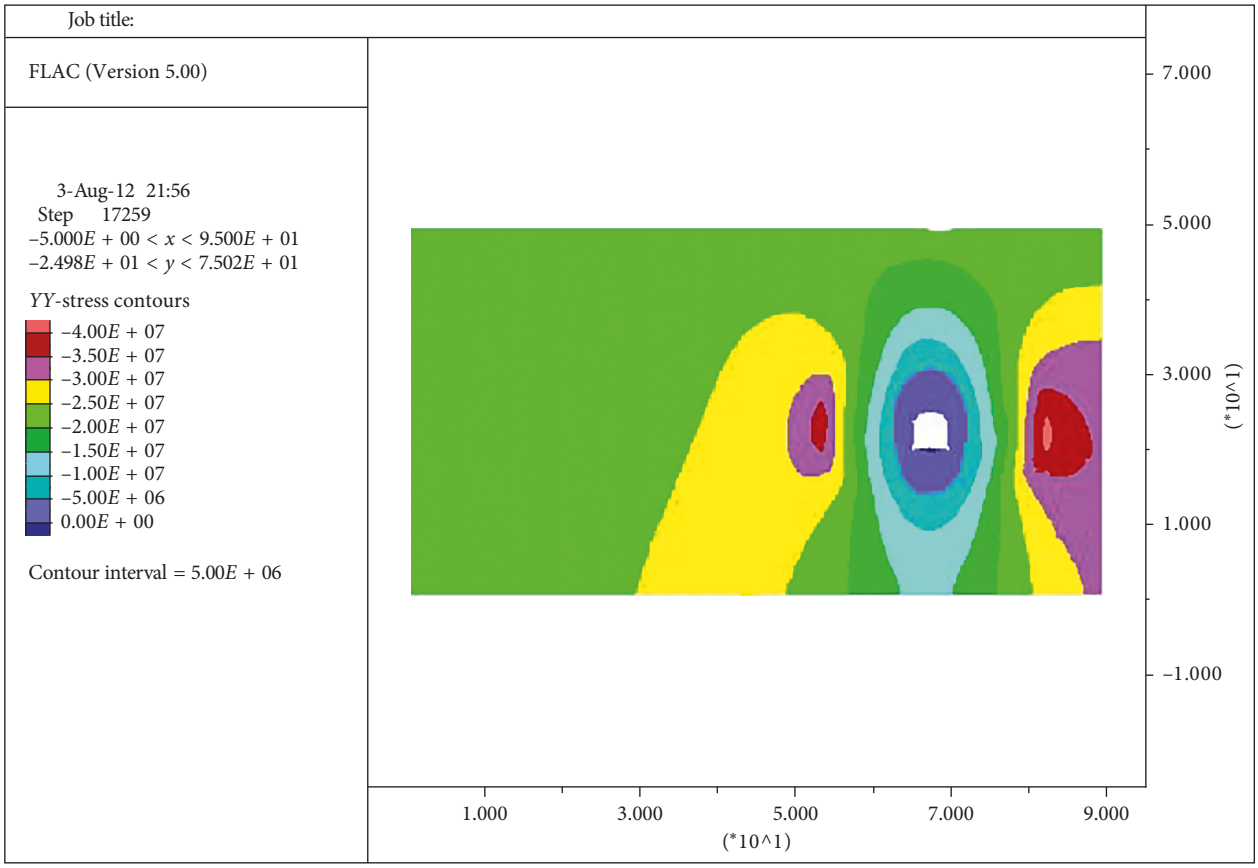

(a)

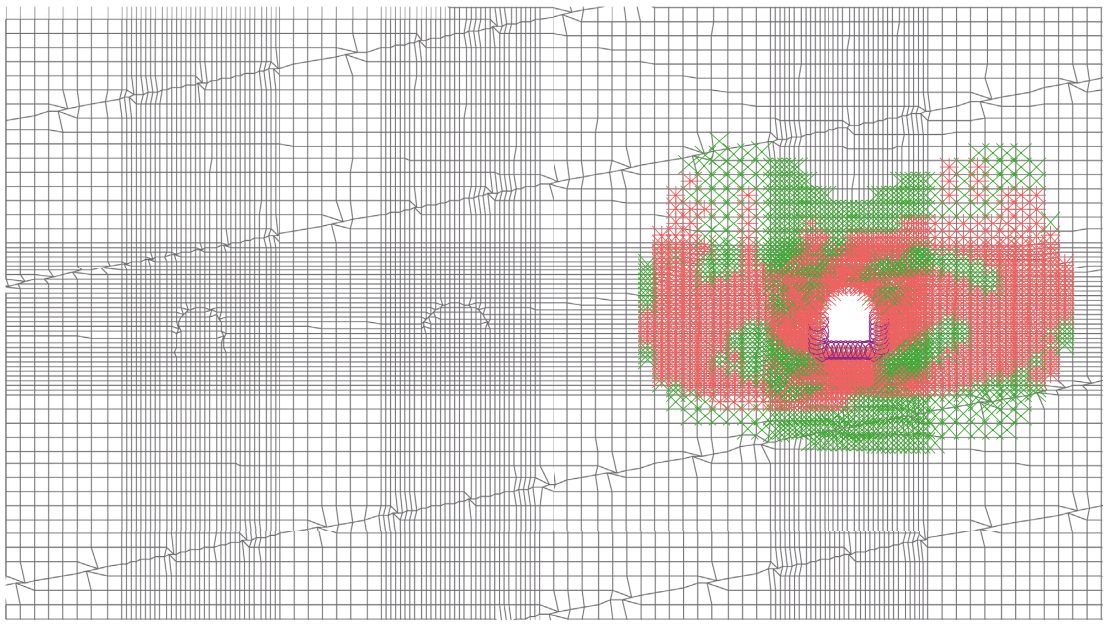

(b)

Figure 5: Calculation results when the excavation of the water pump house alone is done: (a) vertical stress of surrounding rock; (b) plastic zone of surrounding rock.

(4) The support system was adapted to the strong deformation characteristics of the deep surrounding rock. The continuous deformation control effect of large-diameter anchor cable support for elastic deformation, plastic deformation before peak strength, and overall deformation of the anchorage zone

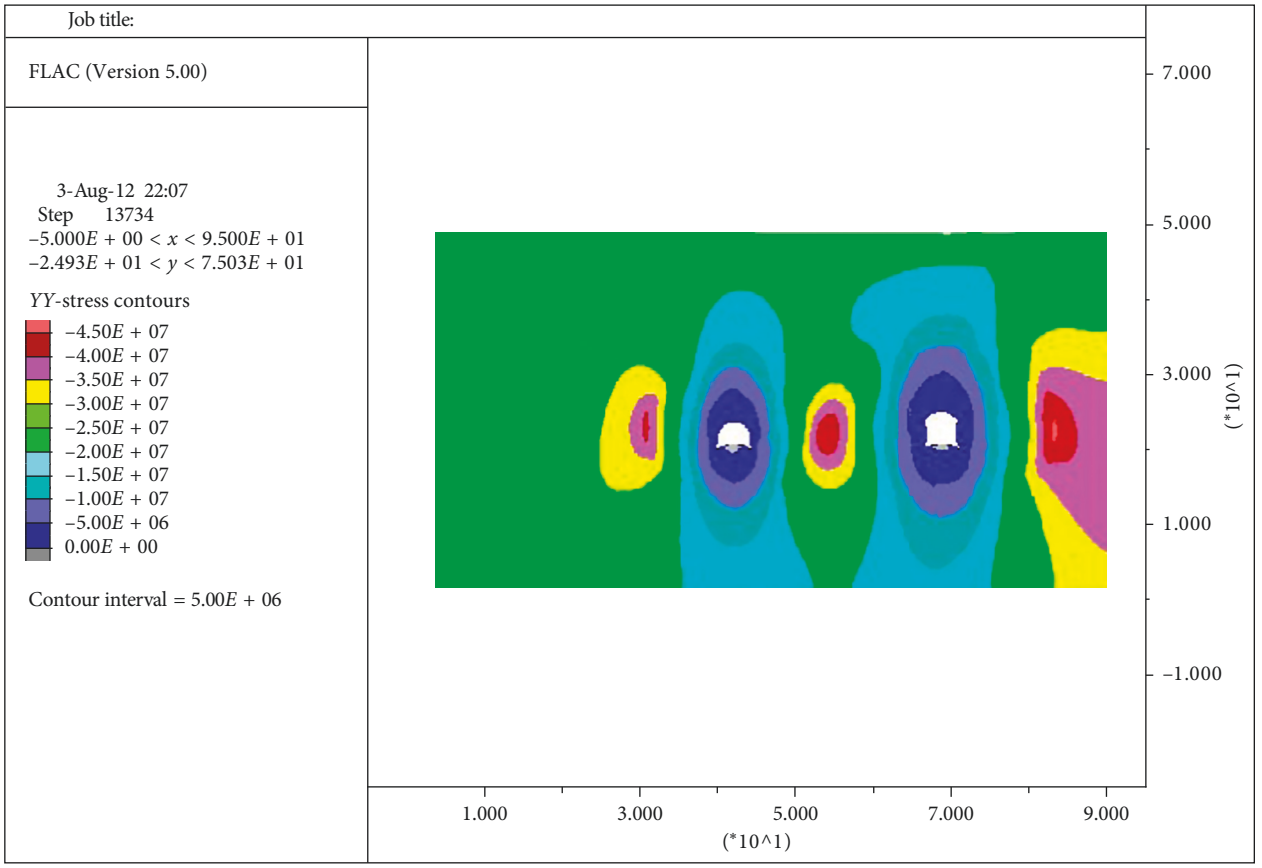

(a)

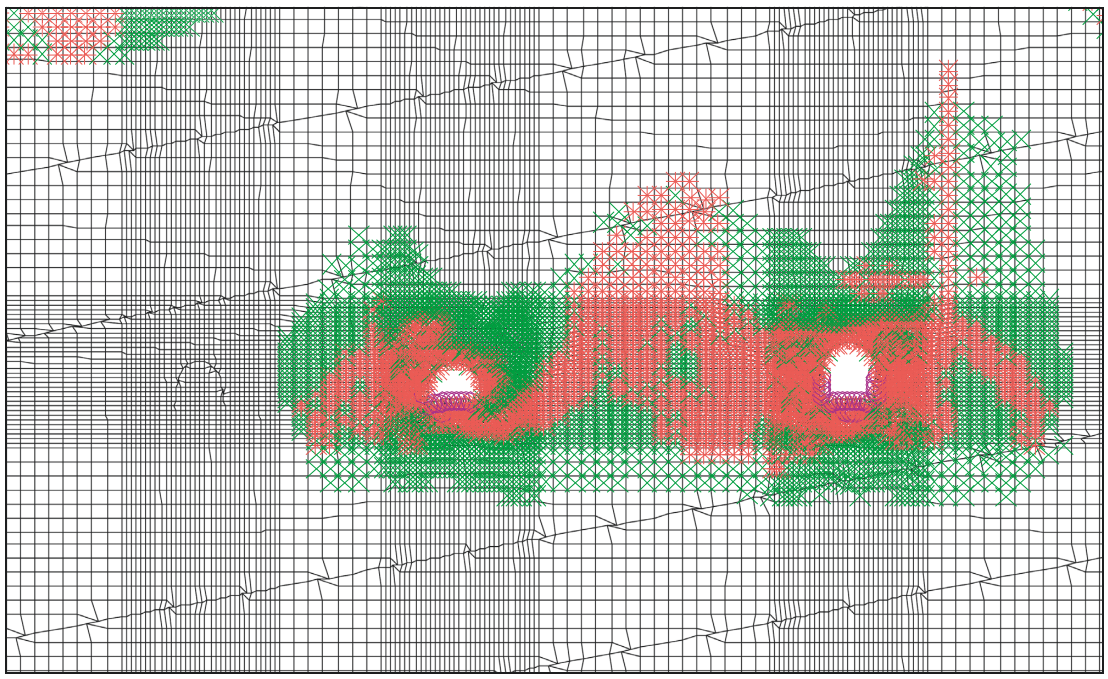

(b)

Figure 6: Calculation results when the excavation of the water pump house and main haulageway at the same time is done: (a) vertical stress of surrounding rock; (b) plastic zone of surrounding rock.

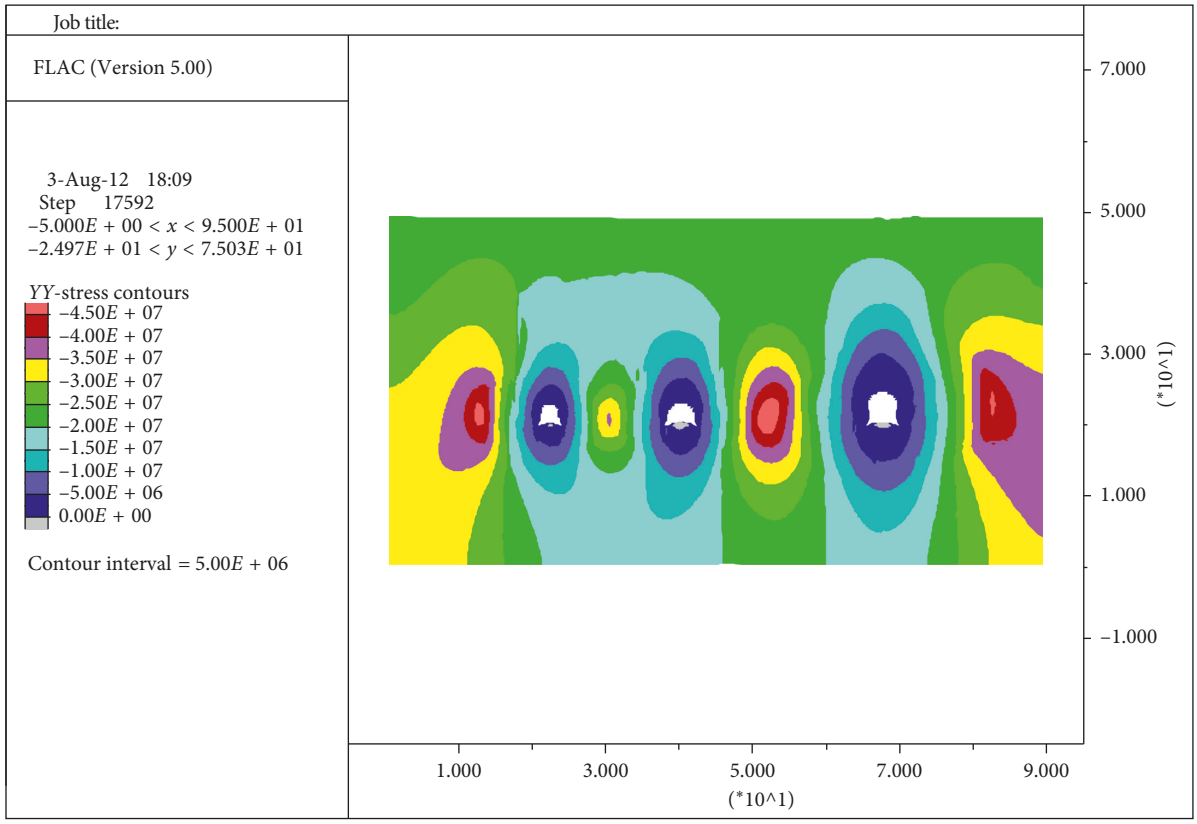

(a)

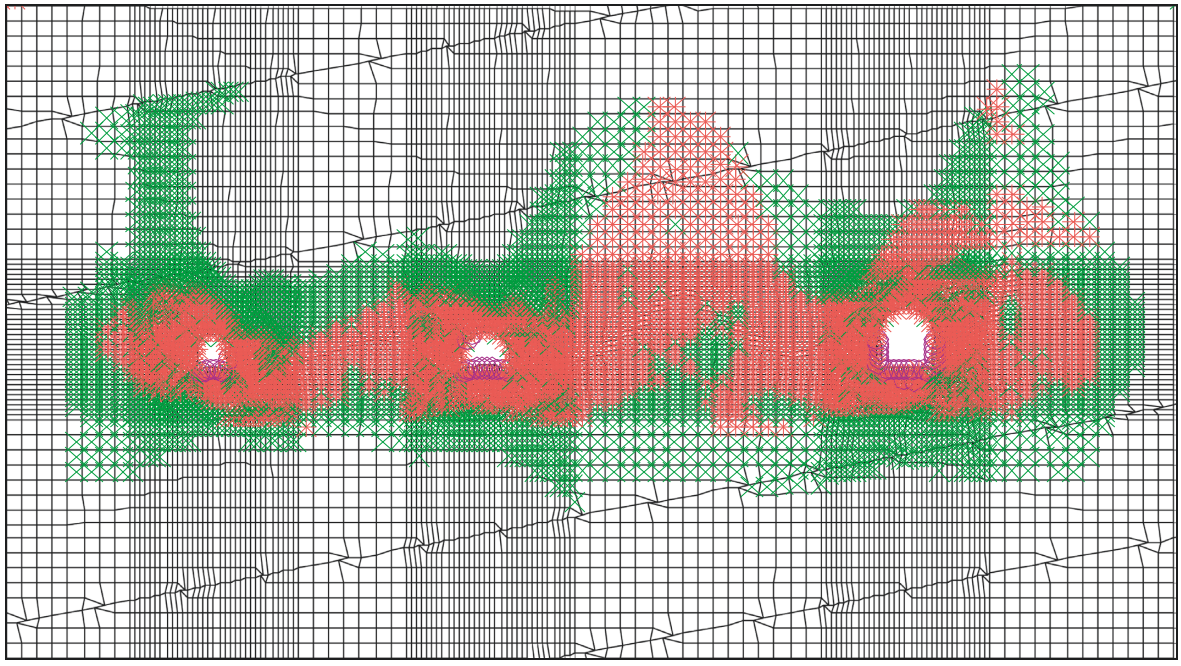

(b)

Figure 7: Calculation results of the excavation of the waiting room, main haulageway, and water pump house at the same time: (a) vertical stress of surrounding rock; (b) plastic zone of surrounding rock.

was not noticeable. The support system was required with sufficient elongation, and the continuous deformation of surrounding rock was released.

(5) The strength and integrity of surrounding rock were entirely enhanced. The combined support technology of the grouting anchor cable was applied, and the

pretightening force of long anchor cable was exerted. Then, the cobearing function of support plus rock mass was regulated, and the self-bearing capacity of slurry improved the self-bearing ability of rock mass. At the same time, the deformation and damage of surrounding rock were adequately controlled by adopting primary support that achieved with the high prestress and the combined support of the strong bolt, and the secondary support and the maintenance of roadway were avoided.

4.2. Key Technologies and Equipment. The deformation of surrounding rock in the chamber and roadway was caused by the floor mainly and the instability and deformation occurred at the beginning of the floor. Therefore, the control of each chamber and roadway was focused on the prevention and control of the floor. Combined anchor cable support was adopted as the control technology of the floor heave. In the specific scheme, use three high prestressed combined cables that length 6~14 m and diameter 17.8 mm, of which the head of the anchor cable was 3 m length and was arranged in beaded (Figure 8). The combination structure of single support with the different performance was adopted at the support method, and the characteristics of various supporting forms were given a play that the requirements of soft rock formation pressure and deformation were adapted and the stability of surrounding rock was achieved ultimately. The deep hole grouting of grouting anchor cable is to squeeze cement mortar into the crack of loose surrounding rock. A high-strength bearing arch was constituted by the fractured rock and cement slurry together that the deformation and pressure of surrounding rock were resisted. The anchoring method was to anchor the long anchor cable into the deep stable rock mass and then the prestress was applied to the anchor cable. According to the direction, size, and the anchorage depth of the design requirement, the active preload stress was preimposed on the rock wall.

The construction technology of combined grouting anchor mainly composed of assembling, drilling, grouting, and prestressing processes. The equipment of special floor anchor cable drill was applied into the combined anchor of the floor. There are several examples of successful applications in China at present; for example, the pneumatic frame column Type Anchor Cable drill for ZQJ-300 was constructed into holes effectively (Figure 9). This equipment can drill and construct the floor anchor and anchor hole in the soft rock roadway, avoiding the phenomenon that collapse, stuck, break the bar, and so on because the deep gravel cannot be eliminated. For the floor drilling, the construction quality was improved, the hole formation rate was increased, the drilling depth was extended, and construction time was shortened, and thus a lot of costs for mine roadway construction were saved.

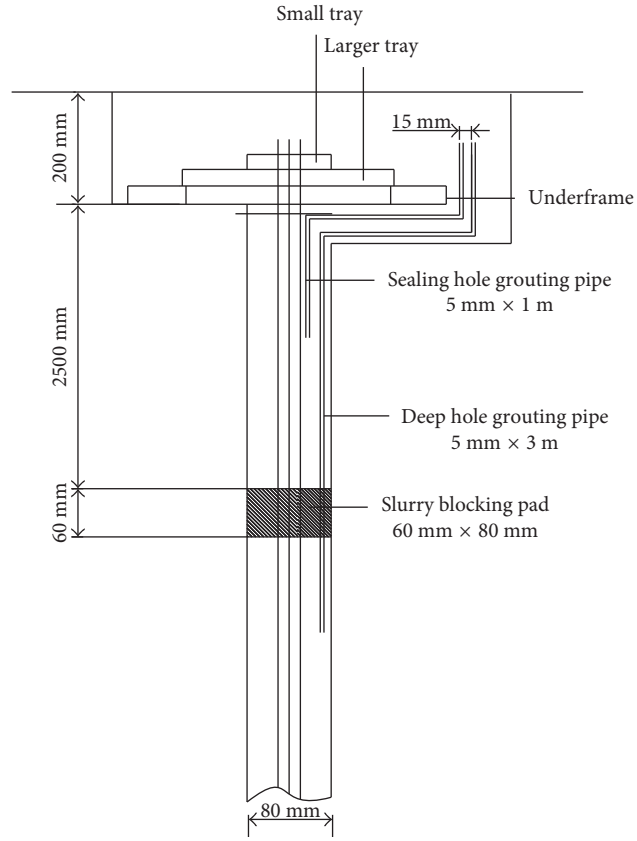

Figure 8: Illustration of combined grouting anchor structure.

Figure 9: Anchor cable rig dedicated by the floor.

5. Comprehensive Control Technology of Chamber (Take Water Pump House as an Example)

5.1. The Overall Design. From the field observation, for water pump house, substation, waiting room, and main

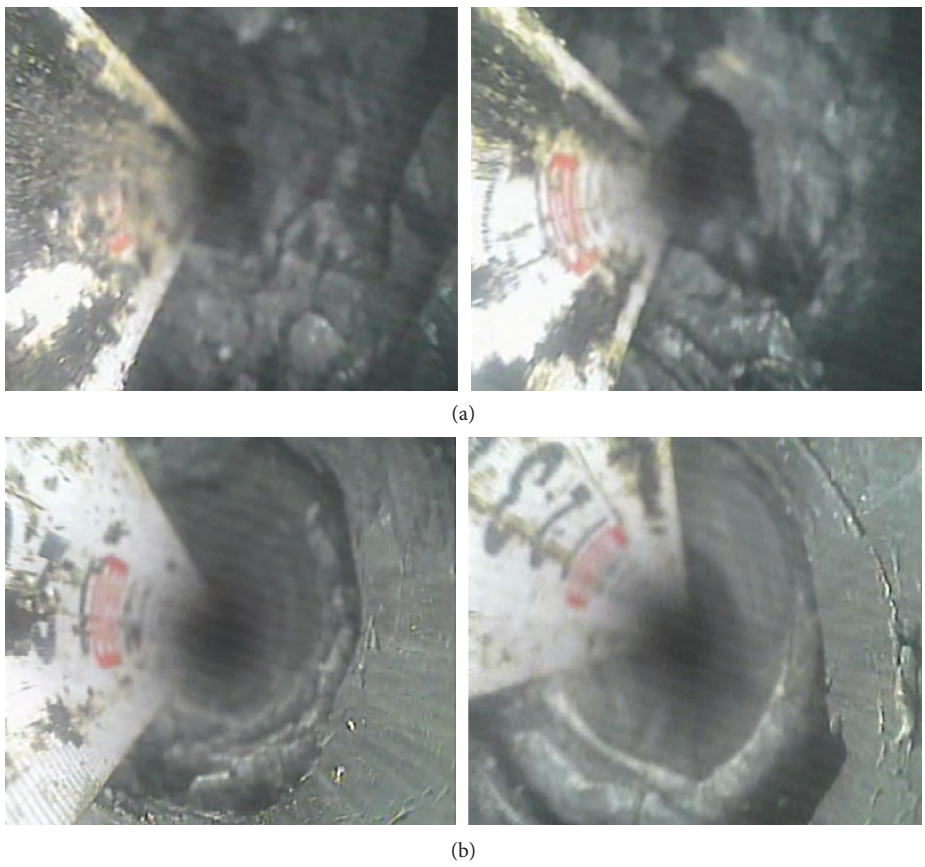

(a)

(b)

Figure 10: Two sides of water pump house surrounding rock peeping results (one hole in each of one side). (a) Broken rock mass. (b) More complete rock mass.

haulageway, the deformation of the chamber was mainly manifested by the heaving of the floor and the sides, especially the floor. Therefore, how to control the floor heaving was the key. According to the surrounding rock conditions observed at the scene, the continuous deformation of the floor and sides rock masses to the roof of the chamber or roadway were caused by the low strength of surrounding rock, high stress, and mutual excavation of chambers. Thus, the high transfer stress to the floor of the chamber was prevented, or the rock mechanics strength of floor and sides was improved firstly at support. The integrated control method of the anchor, metal mesh, grouting, combination cable, and large-diameter anchor was used to the whole section of the water pump house. Besides, the entire section of the chamber was reinforced by grouting, the integrity and strength of surrounding rock were improved, and the support of floor anchor or combined anchor was carried out.

5.2. Internal Damage of Surrounding Rock in Water Pump House Chamber. Three hole peep tests were carried out in the water pump house chamber of the main well bottom yard at the –850 m level, in which two hole peep tests were set in the sides and one set on the top, respectively. The peep test results show that the rock mass of sides from the orifice to the inside of hole about 70~90 cm has integrity, the rock mass in 70~150 cm was broken extremely and still broken in 100~310 cm, cracks appeared in 300~410 cm, and the integrity of rock mass beyond 410 cm was better, respectively. The loosening range was about 4 m (Figure 10). The broken way of the roof and sides was slightly different (Figure 11); the rock mass of the roof has integrity in 0~20 cm inside the hole and was extremely broken in 20~220 cm, broken in 220~250 cm, and cracked in 250 cm~300 cm; and the rock was integrity beyond 300 cm, respectively. Therefore, the loose range of the water pump house was about 3~4 m.

5.3. Grouting Reinforcement. According to the results of the site test, the excavation was performed first and then grouting was carried out to ensure the loose rock mass and the safety of late excavation. The loosening range was about 3.0~4.0 m from the internal fissure structure of surrounding rock. Therefore, the length of grouting hole was designed for 5 m, the spacing was 2000 mm × 1600 mm, the grouting was mainly applied in the roof and sides, and the grouting material was cement-sodium silicate binary slurry. The particular arrangement is shown in Figure 12.

5.4. Bolt Support Parameters. The anchor bolts were mainly arranged in the sides and the roof. The left-handed without longitudinal reinforcement high strength rebar anchorage rod (BHRB500) was used, with a diameter of 22 mm and a length

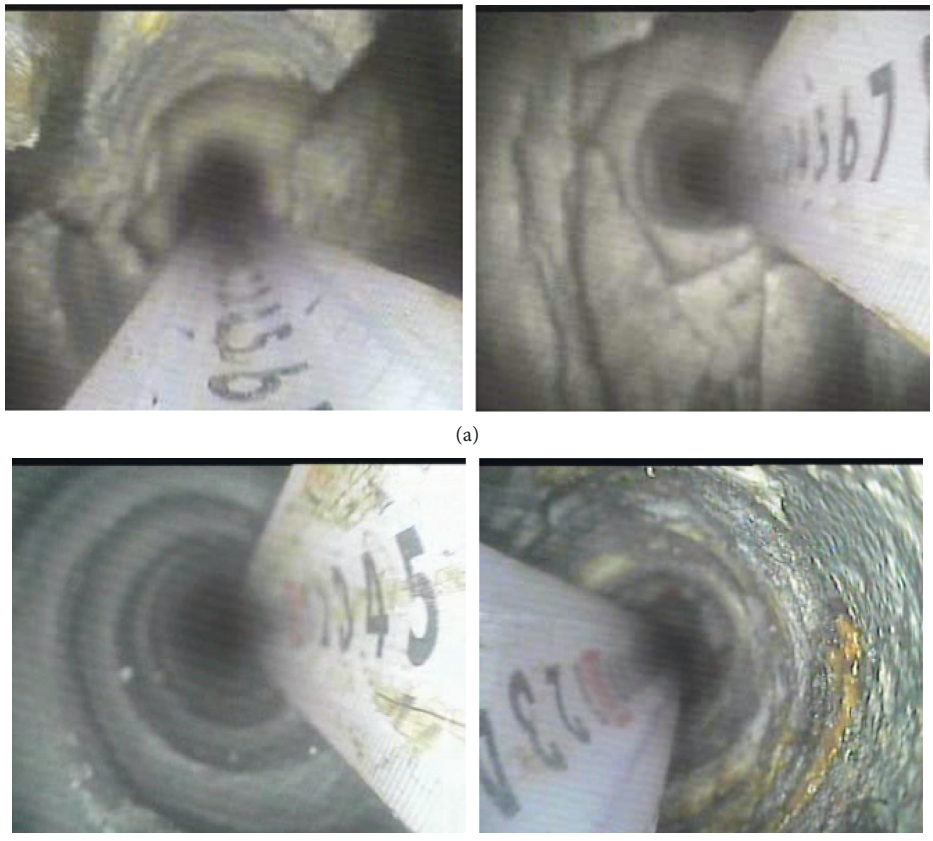

(a)

(b)

Figure 11: The roof of water pump house surrounding rock peeping results. (a) Broken rock mass. (b) More complete rock mass.

of 2600 mm length. Three rolls of K2350-type resin anchoring agents were used for each anchor, the pretightening force was not less than 100 kN, and the spacing was 800 mm × 800 mm (Figure 13). The metal mesh and the reinforced ladder beam were used in full section, in which the diameter and the grid of the metal mesh were 6 mm and 80 mm × 80 mm, respectively. The metal mesh joint must have a bolt and a steel ladder beam to tighten it and stick it close to the rock face. When the length of the mesh is not less than 100 mm, the steel ladder beam is welded by a 12 mm diameter round steel. The anchor bolts were installed with a downward tilt of 15°.

5.5. Large Diameter Anchor Support Parameters. The large-diameter anchor cable is 21.6 mm diameter × 7.3 m length, made of steel strands, and the spacing is 2000 mm × 1600 mm, respectively. (Figure 13). The end of the resin was anchored, and the length of the anchorage was 2000 mm. Five rolls of Z2350-type resin were used in each anchor with the pretightening force not less than 100 kN. The anchor cable stack was superimposed with two pads, and the specifications of the square pillow were 350 mm × 350 mm × 10 mm and 150 mm × 150 mm × 10 mm, respectively, and the big pad was on the small one. The bottom angle anchor was tilted at an angle of 15°~25°downward for installation. Each of the two anchor cables of the chamber was attached as a set of steel strips, and the further deformation of the loose surrounding rock was maintained.

5.6. Combined Grouting Cable Support Parameters. The combination grouting anchor is mainly for the floor; each group is composed of three anchor cables with 17.8 mm diameter × 4000 mm length and the spacing is 2000 mm × 1600 mm. Three sets were designed for each row. The length of grouting anchor was 4 m, divided into anchoring section (2.0 m), free section (1.5 m), and tension section (0.5 m). The whole anchor cable was combined by the steel strand, guide cap, plastic casing, support frame, and exhaust pipe. No.25 U-barl together with a 20 mm steel plate was used for the anchorage plate. The grouting anchor was raised and pulled with the pretightening force not less than 120 kN. The grouting material was cement-water glass double slurry, and the specific layout and parameters are shown in Figure 13.

6. Control Effect of Chamber Rock with the New Support Program

6.1. Numerical Simulation Analysis. The numerical calculation model of anchor bolt support was established with the repair design scheme, and the monitoring results of surrounding rock deformation with the new support scheme are shown in Figure 14 and Table 4, respectively.

After the monitoring of surrounding rock, the deformation of surrounding rock was decreased obviously with the support of high strength bolt, anchor cable, and grouting.

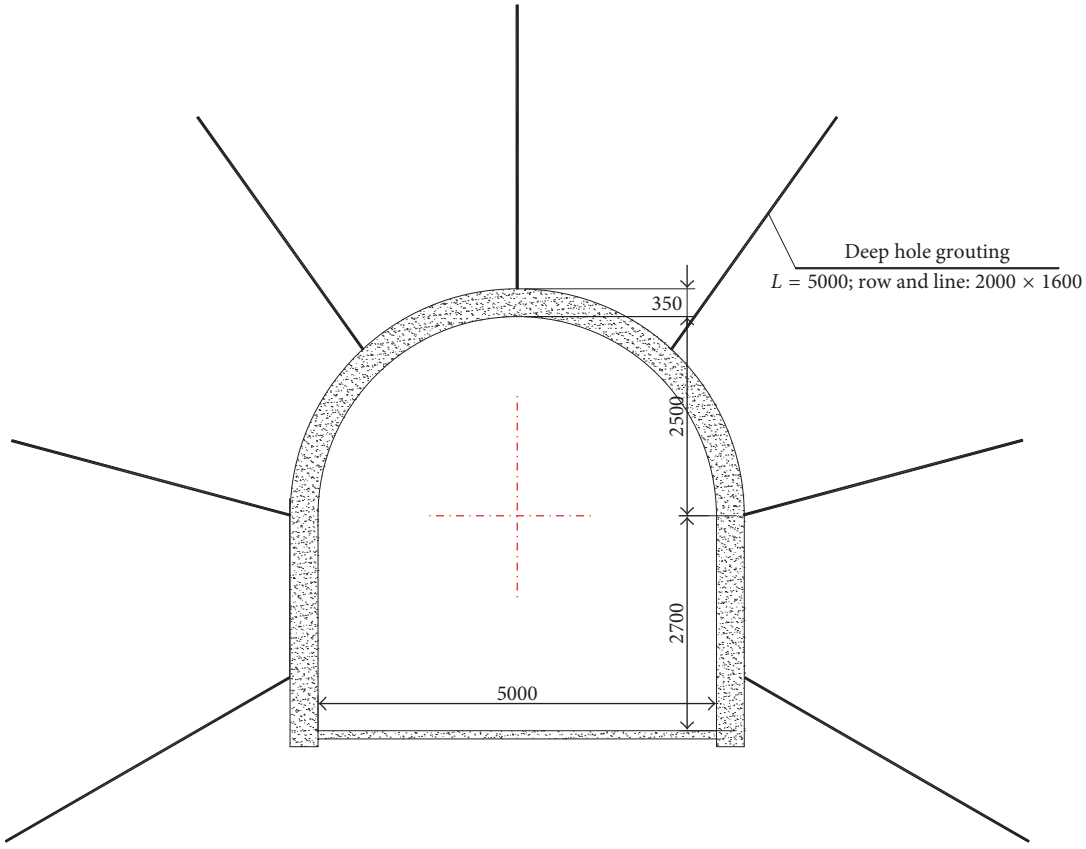

Figure 12: Pregrouting design (unit: mm).

Whether it was the roof-floor or sides, the loosening range was smaller significantly (Figure 15). Also, the support of bolt, anchor cable, and grouting were strengthened, and the anchor cable was anchored in a stable fine sand stratum with the deformation of surrounding rock. The large deformation and the extending range of loose rock were resisted effectively, so that the stress release of rock mass was significantly reduced. Therefore, it can be seen from the stress distribution situation (as shown in Figure 16) that the horizontal stress and vertical stress were less than 7.5 MPa and 15 MPa, respectively. That is, the surrounding rock area at the lower stress level was less than 0.5 times roadway size range, especially the vertical stress at a low level of surrounding rock. However, the deformation of the roadway has been restrained, and the stress around the roadway has concentrated due to the full exertion of the tensile and reinforcement effects of the anchorage cable. The plastic area under strengthening support is shown in Figure 17, and the yield area and destruction range of surrounding rock was reduced, within the control range.

Therefore, the chamber of water pump house, transport lanes, substations, and waiting room in −850 m shaft station of Qujiang Coal Mine were repaired and supported by the integration of the high-strength anchor, high prestressed anchor, and combined grouting anchor, by which the deformation of surrounding rock was adequately controlled.

6.2. Field Monitoring. The deformation of roadway was observed by the interior extrapolation method, and the monitoring curve is shown in Figure 18. After 66 days of monitoring, the average convergence of surrounding rock in sides of the chamber and the average movement of the roof-floor were 27 mm and 42 mm, respectively. The results showed that the modified deformation value of supporting surrounding rock was within the controllable range, all deformations were tended to stabilize at the later stage of monitoring, and the convergence rate was less than 0.2 mm/d. Therefore, the comprehensive control method of the anchor, metal mesh, grouting, combined anchor, and large diameter anchor has dramatically suppressed the rock deformation of the chamber and roadway, and the deformation of the floor heaving was well controlled by the technology of the floor anchor combined with cable support and grouting.

7. Conclusion

(1) The results of numerical calculation showed that the deformation of surrounding rock between the sides and the roof and floor was relatively small while excavating the water pump house alone. While excavating the water pump house and the main haulageway at the same time, the stress distribution was changed by the excavation of the chamber and roadway, especially the excavation of the main

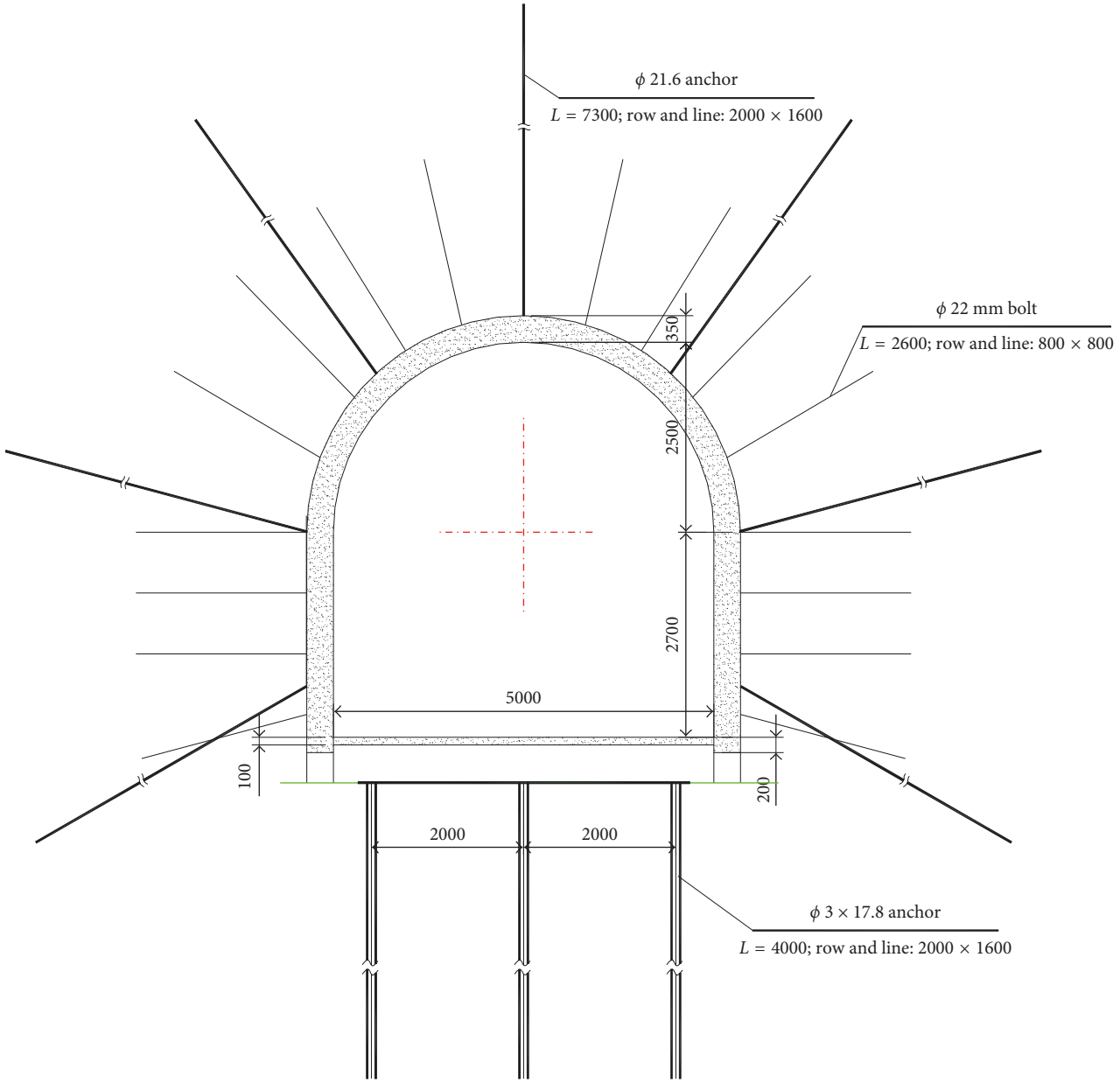

Figure 13: Bolt and anchor support program for the main drainage water pump house chamber.

haulageway, and the convergence of the sides and roof-floor was significantly increased. When the waiting room, main haulageway, and water pump house were all excavated, the deformation of the water pump house was most serious under the influence of excavation disturbance and stress superposition. The left horizontal displacement of the water pump house was higher than the right, a higher stress concentration was formed between the water pump house and the main haulageway, and a more massive horizontal displacement occurred in the chamber near the stress concentration area.

(2) The corresponding control principle was proposed with the deformation characteristics of large deformation soft rock. First of all, the initial support strength of the support system was improved, and the integrity and self-bearing of surrounding rock were maintained. Then, the reasonable prestress was determined by the roadway conditions, the prestress and action scope of the anchor were effectively improved, and the strong deformation characteristics of deep surrounding rock were adapted to the support system. Finally, the strength and integrity of surrounding rock were fully enhanced, and the pretightening effect of the long anchor cable and the self-bearing capacity of rock mass by slurry were strengthened. The cosupporting role of support plus rock mass and the self-bearing capability of rock mass were improved.

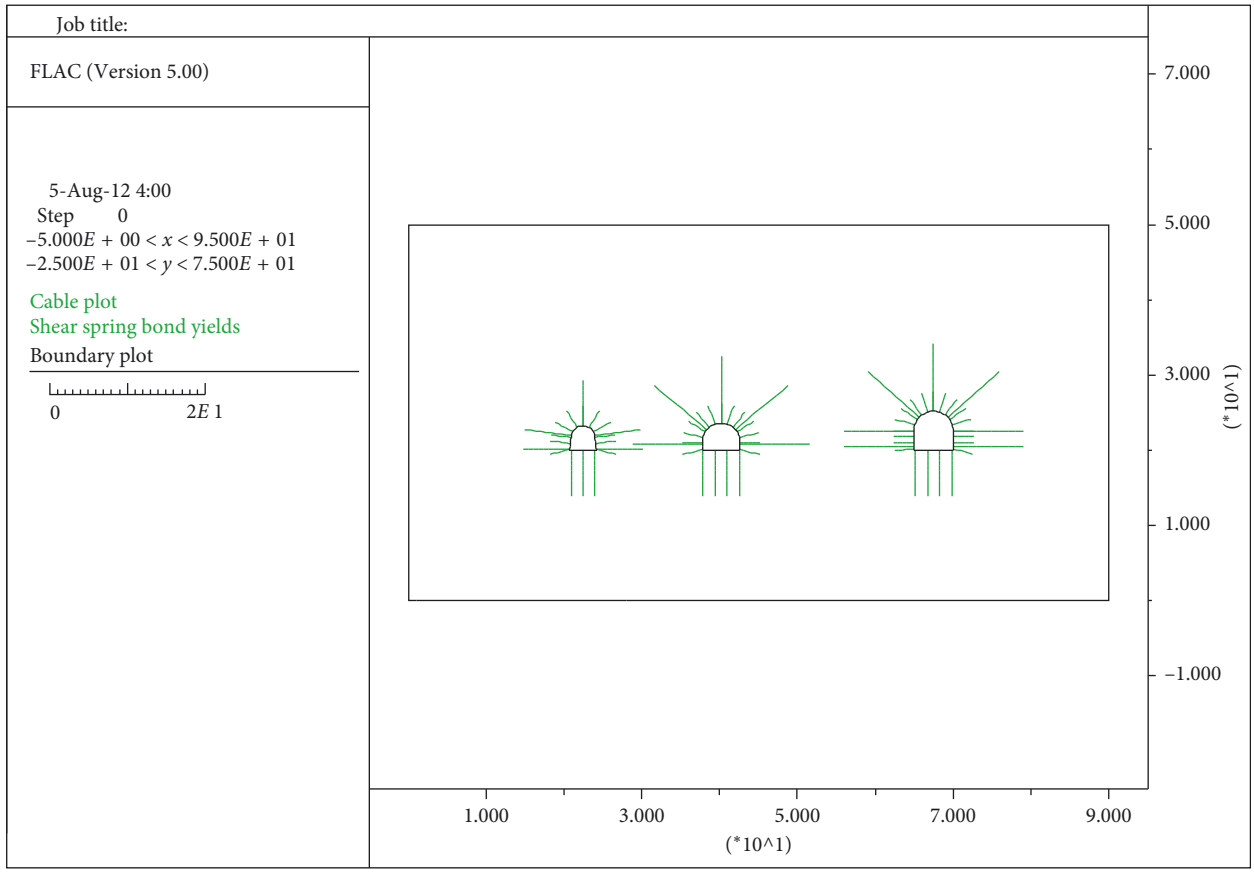

Figure 14: Support simulation model of the anchor and cable.

Table 4: Deformation of surrounding rock of the chamber after adopting the new support scheme (unit: mm).

Chamber type	Floor heave volume	Roof subsidence volume	Left side horizontal displacement	Right side horizontal displacement
Waiting room	124	76	124	149
Water pump house	97	111	175	162
Substation	106	101	134	162

(3) A set of critical technologies and equipment were proposed with the action mechanism of surrounding rock of the high-stress cavern group. One is that the floor deformation of the chamber or roadway was controlled by the supporting technology of the combination anchor cable. A high prestress combined anchor cable that composed of 3 anchorage cables was invented, which had 6~14 m length and 17.8 mm diameter, and the requirements of ground pressure and deformation of soft rock and the stability of surrounding rock were achieved. Second, the drilling hole and construction of the floor anchor and the anchor in the large deformation weak rock roadway were performed by using floor dedicated drilling and anchor installation rig equipment and avoided the phenomenon that collapse, stuck, break the bar, and so on because the deep gravel cannot be eliminated.

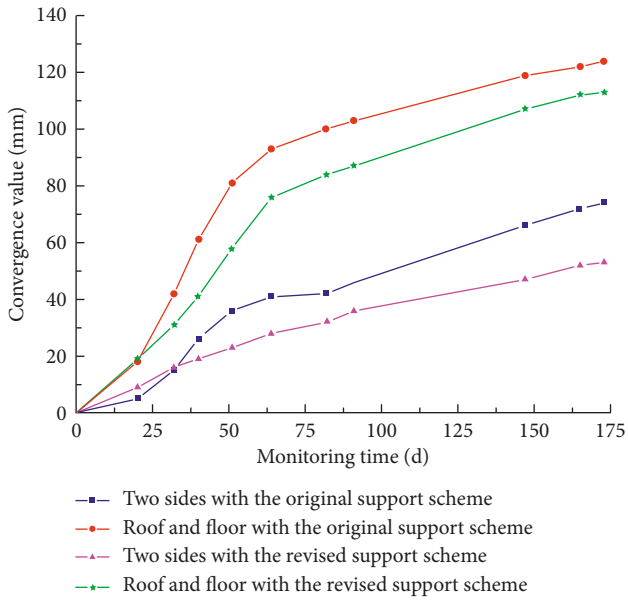

Figure 15: Comparison curve of deformation monitoring.

(4) The comprehensive control method of the bolt, metal net, grouting, combined anchor, and large

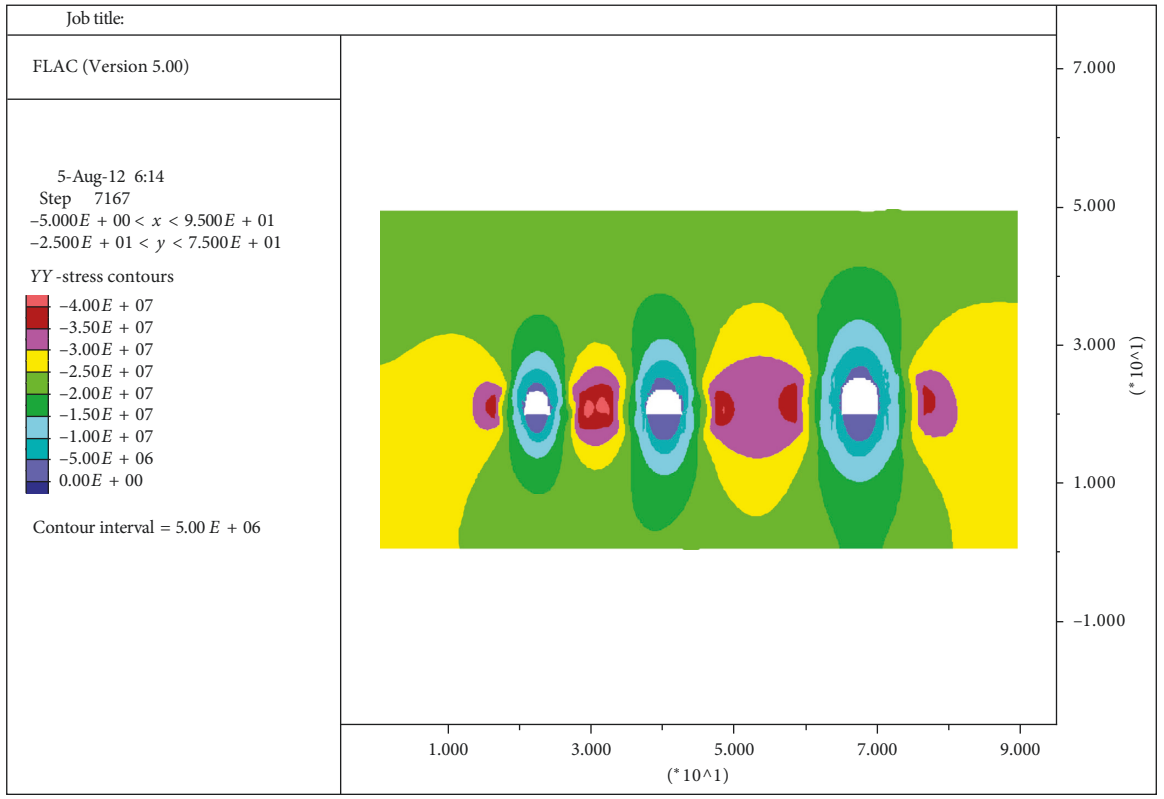

(a)

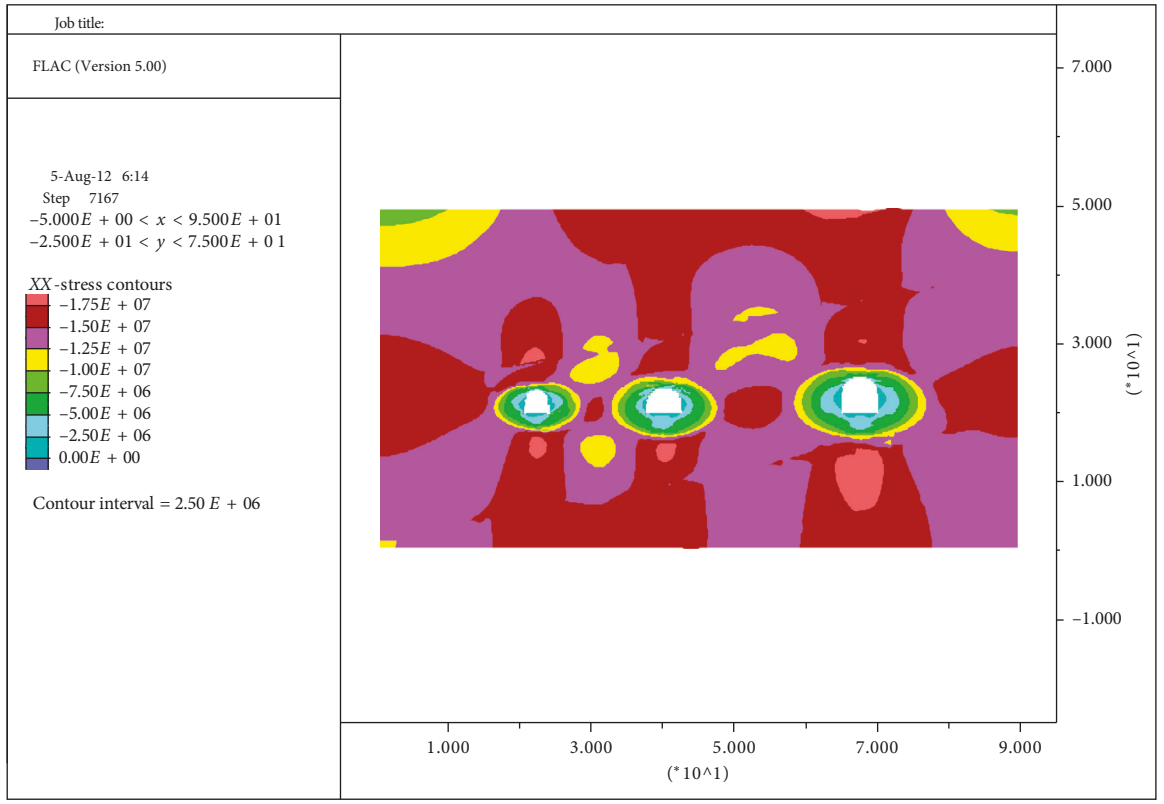

(b)

Figure 16: Surrounding rock stress distribution of each repaired chamber. (a) Vertical stress field. (b) Horizontal stress field.

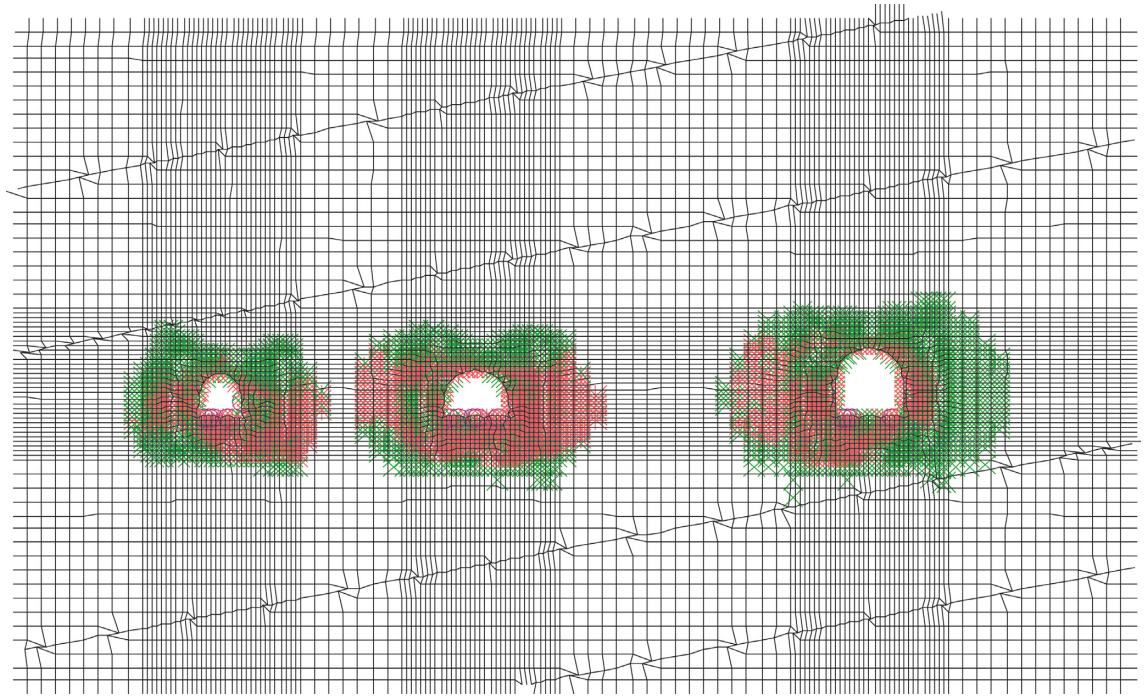

Figure 17: Plastic regions of each repaired chamber.

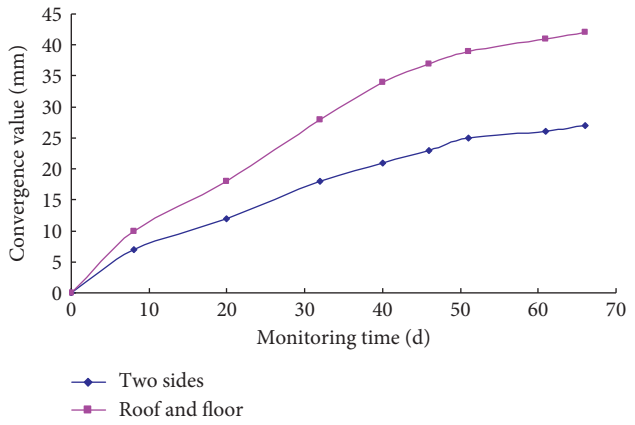

Figure 18: Monitoring curve of the surrounding rock in the chamber of the water pump house.

diameter anchor was put forward, water pump house as an example. And the relevant supporting parameters were determined according to the internal failure of surrounding rock in the chamber. Numerical simulation analysis showed that the surrounding rock deformation of the chamber and roadway was reduced with the modified support scheme. With the deformation of surrounding rock, the anchor cable was anchored in a stable fine sand stratum, and the continuous increase of rock mass loosening range was prevented effectively. The field test showed that the revised convergence rate of supporting rock was less than 0.2 mm/d with the monitoring of 66 days. Therefore, the surrounding rock deformation of the chamber and roadway was effectively prevented by the integrated control method.

Data Availability

The data used to support the findings of this study are included in the article, which are based on the geological data of the site and the data generated during the experiment.

Conflicts of Interest

The authors declare that they have no conflicts of interest.

Acknowledgments

This study was supported by the National Natural Science Foundation of China (51574122, 51434006, and 51774130) and the Open Research Foundation of Key Laboratory of Safety and High-efficiency Coal Mining, Ministry of Education (Anhui University of Science and Technology) (JYBSYS2015201). The financial supports are greatly appreciated.

References

[1] M. K. Hyung, J. Rutqvist, J. H. Jeong, B. H. Choi, D. W. Ryu, and W. K. Song, "Characterizing excavation damaged zone and stability of pressurized lined rock caverns for underground compressed air energy storage," *Rock Mechanics and Rock Engineering*, vol. 46, no. 5, pp. 1113–1124, 2013.

[2] S. Q. Duan, X. T. Feng, Q. Jiang, G. Liu, S. F. Pei, and Y. L. Fan, "In situ observation of failure mechanisms controlled by rock masses with weak interlayer zones in large underground cavern excavations under high geostress," *Rock Mechanics and Rock Engineering*, vol. 50, no. 9, pp. 2465–2493, 2017.

[3] W. J. Yu, S. H. Du, W. J. Wang, and Y. J. Zhu, "Excavation disturbance and stability of short-distance roadway with high stress and soft rock mass," *Chinese Journal of Geotechnical Engineering*, vol. 36, no. 1, pp. 57–64, 2014.

[4] Y. S. A. Loh, S. M. Yidana, B. Banoeng-Yakubo, P. A. Sakyi, M. O. Addai, and D. K. Asiedu, "Determination of the mineral stability field of evolving groundwater in the Lake Bosumtwi impact crater and surrounding areas," *Journal of African Earth Sciences*, vol. 121, no. 2, pp. 286–300, 2016.

[5] P. T. Nhan, G. Zhang, V.-N. Nguyen, and V. H. Le, "Study on the coupling effect between surrounding rock and support structures of tunnels," *Advances and Applications in Geospatial Technology and Earth Resources*, vol. 10, no. 6, pp. 355–366, 2017.

[6] W. J. Yu, W. J. Wang, G. S. Wu, X. Yu, and W. Peng, "Three zones and support technique for large section incline shaft crossing goaf," *Geotechnical and Geological Engineering*, vol. 35, no. 5, pp. 1921–1931, 2017.

[7] K. R. Dhawan, D. Sing, and I. D. Gupta, "Three-dimensional finite element analysis of underground caverns," *International Journal of Geomechanics*, vol. 4, no. 3, pp. 224–228, 2004.

[8] F. S. Ebrahim, N. Majidreza, and A. Giacomini, "A numerical investigation of sinkhole subsidence development over shallow excavations in tectonised weak rocks: the Dolaei Tunnel's excavation case," *Geotechnical and Geological Engineering*, vol. 35, no. 4, pp. 1685–1716, 2017.

[9] J. H. Yang, W. B. Lu, Y. G. Hu, M. Chen, and P. Yan, "Numerical simulation of rock mass damage evolution during deep-buried tunnel excavation by drill and blast," *Rock Mechanics and Rock Engineering*, vol. 48, no. 5, pp. 2045–2059, 2015.

[10] R. S. Yang, H. J. Xue, D. M. Guo, Y. L. Li, and T. T. Li, "Failure mechanism of surrounding rock of large section chambers in complex rock formations and its control," *Journal of China Coal Society*, vol. 40, no. 10, pp. 2234–2242, 2015.

[11] H. L. Lin and Y. K. Shi, "Simulation on stability of surrounding rock of large section chambers in deep structural complex areas," *Journal of China Coal Society*, vol. 36, no. 10, pp. 1619–1624, 2011.

[12] Q. Yang, G. Yang, Z. C. Wang, X. G. Zhu, and M. T. Luan, "Application of block theory to surrounding rock stability of underground caverns in Huanggou pumped storage station," *Chinese Journal of Rock Mechanics and Engineering*, vol. 26, no. 8, pp. 1618–1624, 2007.

[13] Y. L. Zhao, L. Y. Zhang, W. J. Wang, C. Z. Pu, W. Wan, and J. Z. Tang, "Cracking and stress-strain behavior of rock-like material containing two flaws under uniaxial compression," *Rock Mechanics and Rock Engineering*, vol. 49, no. 7, pp. 2665–2687, 2016.

[14] X. M. Sun, D. Wang, C. Y. Miao, Y. Li, and H. C. Xu, "Research on dynamic pressure instability mechanism and control countermeasure of deep pump room and chamber group in Nantun coal mine," *Journal of China Coal Society*, vol. 40, no. 10, pp. 2303–2312, 2015.

[15] Q. Z. Wang, W. B. Xie, S. G. Jing, and X. B. Fei, "Instability mechanism and control technology of chamber group surrounding rock in complex structural area," *Journal of Mining and Safety Engineering*, vol. 31, no. 2, pp. 263–269, 2014.

[16] M. C. He, G. F. Li, A. W. Ren, and J. Yang, "Analysis of the stability of intersecting chambers in deep soft-rock roadway construction," *Journal of China University of Mining and Technology*, vol. 37, no. 2, pp. 167–170, 2008.

[17] H. P. Kang, J. Lin, J. H. Yang, Y. Z. Wu, and F. Q. Gao, "Stress distribution and synthetic reinforcing technology for chamber group with soft and fractured surrounding rock," *Chinese Journal of Geotechnical Engineering*, vol. 33, no. 5, pp. 808–814, 2011.

[18] J. Wang, H. Wang, Z. B. Guo, Y. X. Hao, and J. S. Cui, "Stability control strategy of high stress and intense expansion softrock underground openings for pump house in deep mine," *Journal of Mining and Safety Engineering*, vol. 32, no. 1, pp. 77–82, 2011.

[19] D. W. Yin, S. J. Chen, X. Q. Liu, and H. F. Ma, "Simulation study on strength and failure characteristics for granite with a set of cross-joints of different lengths," *Advances in Civil Engineering*, vol. 2018, Article ID 2384579, 10 pages, 2018.

[20] M. Chen, Y. G. Hu, W. B. Lu, P. Yan, and C. J. Zhou, "Numerical simulation of blasting excavation induced damage to deep tunnel," *Rock and Soil Mechanics*, vol. 32, no. 5, pp. 1531–1537, 2011.